



## Antimicrobial activity of lysozyme isoforms: Key molecular features

Mélanie Derde, Véronique Vie, Astrid Walrant, Sandrine Sagan, Valérie Lechevalier-Datin, Catherine Guérin-Dubiard, Stéphane Pezenne, Marie-Françoise Cochet, G. Paboeuf, Maryvonne Pasco, et al.

### ► To cite this version:

Mélanie Derde, Véronique Vie, Astrid Walrant, Sandrine Sagan, Valérie Lechevalier-Datin, et al.. Antimicrobial activity of lysozyme isoforms: Key molecular features. Biopolymers, 2017, 107 (12), pp.e23040. 10.1002/bip.23040 . hal-01593208

**HAL Id: hal-01593208**

**<https://hal.science/hal-01593208>**

Submitted on 16 Feb 2023


**HAL** is a multi-disciplinary open access archive for the deposit and dissemination of scientific research documents, whether they are published or not. The documents may come from teaching and research institutions in France or abroad, or from public or private research centers.

L'archive ouverte pluridisciplinaire **HAL**, est destinée au dépôt et à la diffusion de documents scientifiques de niveau recherche, publiés ou non, émanant des établissements d'enseignement et de recherche français ou étrangers, des laboratoires publics ou privés.



Distributed under a Creative Commons Attribution - ShareAlike 4.0 International License

# Antimicrobial activity of lysozyme isoforms: Key molecular features

Melanie Derde<sup>1</sup> | Véronique Vié<sup>2</sup> | Astrid Walrant<sup>3</sup> | Sandrine Sagan<sup>3</sup> |  
Valérie Lechevalier<sup>1</sup> | Catherine Guérin-Dubiard<sup>1</sup> | Stéphane Pezenec<sup>1</sup> |  
Marie-Françoise Cochet<sup>1</sup> | Gilles Paboeuf<sup>2</sup> | Maryvonne Pasco<sup>1</sup> |  
Florence Baron<sup>1</sup> | Michel Gautier<sup>1</sup> | Sophie Jan<sup>1</sup> | Françoise Nau<sup>1</sup> 

<sup>1</sup>STLO, UMR1253, Agrocampus Ouest, INRA, Rennes, F-35, France

<sup>2</sup>Université de Rennes 1, Institut de Physique de Rennes, UMR6251, CNRS, Rennes, F-35, France

<sup>3</sup>Sorbonne Universités, UPMC Université Paris 06, PSL Research University, Ecole Normale Supérieure, CNRS, Laboratoire des Biomolécules (LBM), Paris, F-75, France

## Correspondence

Françoise Nau, STLO, UMR1253, Agrocampus Ouest, INRA, F-35 Rennes, France.

Email: francoise.nau@agrocampus-ouest.fr

## Funding information

Conseil Régional de Bretagne

## Abstract

Increasing bacterial resistance towards antibiotics has stimulated research for novel antimicrobials. Proteins acting on bacterial membranes could be a solution. Lysozyme has been proven active against *E. coli* by disruption of both outer and cytoplasmic membranes, with dry-heating increasing lysozyme activity. Dry-heated lysozyme (DH-L) is a mixture of isoforms (isoaspartyl, native-like and succinimide lysozymes), giving rise to two questions: what effects does each form have, and which physicochemical properties are critical as regards the antibacterial activity? These issues were investigated by fractionating DH-L, analyzing structural properties of each fraction, and testing each fraction in vivo on bacteria and in vitro on membrane models. Positive net charge, hydrophobicity and molecular flexibility of the isoforms seem key parameters for their interaction with *E. coli* membranes. The succinimide lysozyme fraction, the most positive, flexible and hydrophobic, shows the highest antimicrobial activity, induces the strongest bacterial membrane disruption and is the most surface active on model lipid monolayers. Moreover, each fraction appears less efficient than DH-L against *E. coli*, indicating a synergetic cooperation between lysozyme isoforms. The bacterial membrane modifications induced by one isoform could facilitate the subsequent action of the other isoforms.

## KEYWORDS

bacterial membrane, dry-heating, lipid monolayer, permeabilization, succinimide lysozyme

**Abbreviations:** AMP, antimicrobial peptide or protein; CA, cardiolipin; CMEC, *E. coli* cytoplasmic phospholipid mixture; DH-L, dry-heated lysozyme; DiSC3, 3, 3'-dipropylthiadicarbocyanine iodide; DOPE, 1,2-di-(9Z-octadecenoyl)-sn-glycero-3-phosphoethanolamine; DOPG, 1,2-di-(9Z-octadecenoyl)-sn-glycero-3-phospho-(1'-rac-glycerol); DPPE, 1,2-dihexadecanoyl-sn-glycero-3-phosphoethanolamine; DPPG, 1,2-dihexadecanoyl-sn-glycero-3-phospho-(1'-rac-glycerol); HEPES, 4-(2-hydroxyethyl)-1-piperazineethanesulfonic acid; HP-nitrocefin, hydrolysis product of nitrocefin; ISO-L, fraction enriched in isoaspartyl lysozyme; LPS, lipopolysaccharide; N-L, native lysozyme; NL-L, fraction enriched in native-like lysozyme; ONP, ortho-nitrophenol; ONPG, ortho-nitrophenylgalactoside; SUC-L, fraction enriched in succinimide lysozyme; TSB, tryptic soy broth.

## 1 | INTRODUCTION

Antimicrobial resistance is an enormous public health problem caused by decades of misuse of the antimicrobial compounds. This results in difficult and expensive disease treatments caused by several pathogens.<sup>[1]</sup> Research for novel antimicrobial compounds is thus needed. These antimicrobial compounds should ideally act on generalized cell targets to limit and/or slow down resistance development. Antimicrobial peptides or proteins (AMP) answer this criterion by acting on the bacterial cell membranes. AMP are mostly cationic, amphiphilic, flexible, and contain a significant proportion of hydrophobic residues.<sup>[2]</sup> These

specific physicochemical properties influence their ability to disrupt the bacterial cell membranes.<sup>[2]</sup>

One of the widely studied antimicrobial proteins is hen egg white lysozyme. This small protein of 123 amino acid residues is mostly known for its hydrolase activity on the peptidoglycan of Gram-positive bacteria. However, several research groups have recently shown lysozyme activity on Gram-negative species such as *E. coli*.<sup>[3–5]</sup> One of the lysozyme mechanisms of action against the Gram-negative bacteria is membrane disruption.<sup>[3,6]</sup> Thus, our group recently established that lysozyme is able to permeabilize the outer and inner membranes of *E. coli*, with and without pore formation, respectively.<sup>[4]</sup>

However, the effect of native lysozyme on the *E. coli* population remains limited to growth latency.<sup>[4]</sup> Therefore, several modifications such as enzymatic hydrolysis,<sup>[7]</sup> fusion with chemical moieties,<sup>[8–10]</sup> and heat-denaturation<sup>[11]</sup> were proposed to enhance the effect of lysozyme. In our laboratory, the effect of dry-heating (heating of lysozyme powder for 7 days at 80°C) has been recently investigated. This process proved to increase the effect of lysozyme on the *E. coli* outer and cytoplasmic membranes.<sup>[4]</sup> Dry-heated lysozyme induces larger and/or more pores in the outer membrane than native lysozyme, it disrupts the membrane potential more efficiently, and it induces stronger potassium leakage out of the bacteria cell.<sup>[4]</sup> Using membrane lipid monolayers as models of the *E. coli* outer (LPS monolayer) and cytoplasmic (CMEC monolayer) membranes, we could show that dry-heating increases the lysozyme affinity for the monolayers and/or its insertion capacity, resulting in lipid packing modifications.<sup>[12,13]</sup>

It can be assumed that these stronger effects on the bacterial membranes are due to the modifications of the physicochemical characteristics of dry-heated lysozyme compared to native lysozyme. Namely, higher positive net charge, hydrophobicity, and flexibility could be at the origin of higher surface-activity.<sup>[14,15]</sup> But dry-heated lysozyme is a mixture of three different isoforms: isoaspartyl lysozyme, native-like lysozyme, and succinimide lysozyme.<sup>[14]</sup> Then, an interesting issue is to know if the different isoforms act distinctively on *E. coli* membranes, and to determine which physicochemical features are decisive.

Isoaspartyl lysozyme and succinimide lysozyme differ from native lysozyme in the primary protein structure. One up to five aspartate or asparagine residues (Asp18, Asp48 or Asp52, Asp66, Asp101, and potentially Asn103) are changed into isoaspartate or succinimide residues for isoaspartyl lysozyme and succinimide lysozyme, respectively.<sup>[14]</sup> Succinimide lysozyme is also more basic and more hydrophobic than native lysozyme, while isoaspartyl lysozyme is more acidic than native lysozyme.<sup>[14]</sup> Native-like lysozyme is a lysozyme isoform which does not differ in apparent net charge from native lysozyme (same retention time on cation exchange chromatography), but of which interfacial properties are increased.<sup>[15]</sup>

To investigate the activity of the individual isoforms on the *E. coli* membranes is then justified, because of the particular physicochemical characteristics of each isoform and thus possible specific protein/membrane interactions. In the presently reported study, a comparison is performed between dry-heated lysozyme and fractions enriched in

each isoform. To get a complete picture of the protein/membrane interactions, experiments were performed *in vivo* and *in vitro*. This mixed approach gives information in the complex system of the living bacterial cell combined with the power of simple model systems to resolve the molecular mechanisms such as lipid/protein interactions.

## 2 | MATERIALS AND METHODS

### 2.1 | Materials

Native lysozyme (N-L) powder (pH 3.2) was obtained from Liot (Annezin, 62-France); it was heated for 7 days at 80°C in hermetically closed glass tubes to obtain dry-heated lysozyme (DH-L). Tris base, potassium phosphate monobasic, potassium phosphate dibasic, ortho-nitrophenylgalactoside (ONPG), 3,3'-dipropylthiadicarbocyanine iodide (DiSC<sub>3</sub>), 4-(2-hydroxyethyl)-1-piperazine-ethane-sulfonic acid (HEPES) and glucose were obtained from Sigma-Aldrich (Saint-Quentin, France). Nitrocefin, casein peptone and yeast extract were obtained from Merck Chemicals (Darmstadt, Germany). Tryptic soy broth (TSB) was purchased from AES (Bruz, France).

The *E. coli* K12 lipopolysaccharides (LPS) were obtained from Invivogen (Toulouse, France) and solubilized at 0.5 g L<sup>-1</sup> in 2:1 chloroform/methanol mixture. A mixture of different lipids (Avanti Polar Lipids, Alabaster, USA) was prepared at 0.25 mM in 2:1 chloroform/methanol mixture to mimic the cytoplasmic membrane of *E. coli* (CMEC) as described by Lugtenberg and Peters;<sup>[16]</sup> it contained 2.6% 1,2-di-(9Z-octadecenoyl)-sn-glycero-3-phospho-(1'-rac-glycerol) (DOPG), 3.9% 1,2-dihexadecanoyl-sn-glycero-3-phospho-(1'-rac-glycerol) (DPPG), 11.8% cardiolipin (CA), 32.3% 1,2-di-(9Z-octadecenoyl)-sn-glycero-3-phosphoethanolamine (DOPE) and 49.4% 1,2-dihexadecanoyl-sn-glycero-3-phosphoethanolamine (DPPE).

### 2.2 | Bacterial strains

*Escherichia coli* K12 was obtained from Institut Pasteur (Paris, 75-France). *Escherichia coli* ML-35p (LacI<sup>-</sup> LacY<sup>-</sup> LacZ<sup>+</sup>, plasmid pBR322) was kindly provided by D. Destoumieux-Garzon (UMR 5119, Ecologie des systèmes marins côtiers, University of Montpellier, France), and initially supplied by R. Lehrer (Department of Medicine, UCLA, USA). *E. coli* ML-35p is lactose permease deficient, and expresses  $\beta$ -lactamase and  $\beta$ -galactosidase in the periplasm and cytoplasm, respectively.

### 2.3 | Preparation of enriched fractions of lysozyme isoforms

The different isoforms of lysozyme generated by dry-heating were purified from DH-L by cation exchange liquid chromatography (CEC). DH-L solution (2 g L<sup>-1</sup>) was prepared in 60 mM phosphate buffer, pH 7.0, and injected onto an S-HYPERD F column (Biosepra, Pall corporation, St-Germain-en-Laye, France) previously equilibrated with the same buffer, using a Varian ProStar chromatography system (Spectra-lab Scientific, Markham, Canada). Elution was performed using a NaCl gradient from 0 to 0.5 M in 180 min, in a 60 mM phosphate buffer pH 7.0 at 10 mL min<sup>-1</sup>. Protein detection was followed by

spectrophotometry at 280 nm (Varian Prostar UV/VIS detector, Spectralab Scientific, Markham, Canada). Three different protein fractions were collected: isoaspartyl lysozyme fraction (ISO-L), native-like lysozyme fraction (NL-L) and succinimide lysozyme fraction (SUC-L). The pH of the SUC-L fraction was adjusted to 4.0 immediately after elution in order to avoid succinimide rings hydrolysis. All the protein fractions were then dialyzed using a cellulose membrane with a molecular weight cut off of 3500 Da (Cellu-Sep T1, TX) and lyophilized using a lyophilizer S.G.D. Serial Cirp CS 10–0.8 (Serial, Le Coudray Saint Germer, France).

The composition of each collected fraction was determined by cation exchange high pressure liquid chromatography (CE-HPLC) using a device consisting of a Waters 2695 separation module and a Waters 2487 dual absorbance detector. The column used was an S-HYPERD 10 (Biosepra, Pall, St-Germain-en-Laye, France). Elution was performed using a NaCl gradient from 0 to 1 M in 44 min, in a 20 mM sodium acetate buffer pH 5.0 at 1 mL min<sup>−1</sup>, as described by Desfougères et al.<sup>[14]</sup> The absorbance of the eluent was followed at 214 and 280 nm. The relative proportion of each protein isoform was estimated from the area corresponding to each peak as determined by the Empower 2 software.

## 2.4 | Fluorescence measurements

Fluorescence measurements were carried out on a Horiba Jobin-Yvon Fluorolog 3 spectrofluorimeter using a 1-cm path length quartz cell. Four μM lysozyme solutions were prepared in 10 mM phosphate buffer pH 7.0. Intrinsic tryptophan fluorescence measurements were recorded in triplicate between 305 and 410 nm after excitation at 295 nm. For 8-anilino-1-naphthalene sulfonate (ANS) fluorescence experiments, ANS was added to the lysozyme samples to reach a final ANS concentration of 120 μM, before spectra were recorded in triplicate, between 420 and 600 nm, after excitation at 390 nm.

## 2.5 | Circular dichroism

Circular dichroism (CD) spectra were recorded in triplicate at 100 nm min<sup>−1</sup> and 20°C on a Jasco 815 (Jasco, Bouguenais, France) spectropolarimeter equipped with a thermostated cell holder, using a 2-mm path length quartz cell. Lysozyme solutions were prepared in 10 mM phosphate buffer pH 7.0 to reach final protein concentrations of 119 and 11.9 μM for near and far UV measurements, respectively. The mean residue ellipticity ([θ]MRW) was calculated using the Equation 1:

$$[\theta]_{MRW} = (\theta_{obsd}MRW)/(10lc) \quad (1)$$

where  $\theta_{obsd}$  is the observed ellipticity in degrees, MRW is the mean residue molecular weight (111.8 g mol<sup>−1</sup> for lysozyme),  $l$  is the path length in centimeters, and  $c$  is the protein concentration in grams per milliliter.

## 2.6 | Fourier transformed infrared spectroscopy

Attenuated total reflectance FTIR spectra were measured from powder samples at a 4 cm<sup>−1</sup> resolution. The spectrophotometer (Bruker Tensor 27) was equipped with a monoreflexion germanium ATR plate

(MIRacle, Pike) and a liquid-nitrogen-cooled mercury-cadmium-telluride detector (Bruker). For each sample, 256 scans were averaged and corrected automatically for water vapor contribution and CO<sub>2</sub>, using Opus software. In addition, the spectra were truncated between 1900 and 1360 cm<sup>−1</sup>, then corrected for overall intensity variations, linear baseline drifts and variations in the contribution of liquid water using extended multiplicative scatter correction.<sup>[17]</sup>

## 2.7 | Nano differential scanning calorimetry (nano-DSC)

DSC experiments were performed on a TA instruments NanoDSC calorimeter. Samples were scanned between 40 and 100°C using a scanning rate of 2°C min<sup>−1</sup>. Lysozyme samples were prepared at 1 mg mL<sup>−1</sup> protein concentration in 5 mM HEPES, pH 7.0, 150 mM NaCl, immediately before use. Samples were passed through a 0.2 μm filter to avoid the presence of aggregates, and protein concentration was checked by measuring the absorbance at 280 nm. DSC scans were analyzed using NanoAnalyze software (TA instruments) and fitted with a two-state scaled model.

## 2.8 | *Escherichia coli* growth assays

Growth assays were performed based on the method described by Derde et al.<sup>[4]</sup> The *E. coli* K12 cultures were grown overnight (18 h) at 37°C under stirring (130 rpm) in TSB in order to obtain about 10<sup>9</sup> CFU mL<sup>−1</sup> *E. coli*. Four tenfold serial dilutions in LB05 (Luria Broth containing 10 g L<sup>−1</sup> peptone of casein, 5 g L<sup>−1</sup> yeast extract, and 0.5 g L<sup>−1</sup> NaCl) were applied on these cultures to obtain 10<sup>5</sup> CFU mL<sup>−1</sup> bacterial suspensions. Lysozyme solutions, previously prepared in demineralized water (3.7 g L<sup>−1</sup> N-L fraction, 3.7 g L<sup>−1</sup> DH-L fraction, 0.19 g L<sup>−1</sup> ISO-L fraction, 1.9 g L<sup>−1</sup> NL-L fraction or 1.7 g L<sup>−1</sup> SUC-L fraction), were added to the bacterial suspension, before incubation at 37°C under stirring (130 rpm). For the control sample, only demineralized water was added to the bacteria suspension before incubation. Cell counting was performed after 2 h as previously described by Baron et al.<sup>[18]</sup> The results for cell counts were based on nine replicates (three biological replicates, each with three technical replicates).

## 2.9 | Outer and cytoplasmic membrane permeability measurements

Outer and cytoplasmic membrane permeability was measured using the Lehrer method,<sup>[19]</sup> modified as described by Derde et al.<sup>[3]</sup> Briefly, the *E. coli* ML-35p culture was grown in TSB containing 50 μg mL<sup>−1</sup> ampicilline at 37°C. After twice-washed in 50 mM Tris-HCl buffer pH 7.0, the bacterial culture was diluted in lysozyme solutions (3.7 g L<sup>−1</sup> DH-L, 0.19 g L<sup>−1</sup> ISO-L, 1.9 g L<sup>−1</sup> NL-L, or 1.7 g L<sup>−1</sup> SUC-L) to obtain about 10<sup>7</sup> CFU mL<sup>−1</sup> bacteria suspensions.

To test outer membrane permeability, 0.015 g L<sup>−1</sup> nitrocefin was added to each sample solution. The outer membrane permeabilization was revealed by nitrocefin hydrolysis due to the periplasmic β-lactamase. The hydrolysis product of nitrocefin (HP-nitrocefin) was

detected by absorbance measurement at 486 nm (Multiscan Go, Thermo Fisher Scientific, Illkirch, France) at 37°C under stirring for 30 min from nitrocefin addition. The maximal velocity of the enzymatic reaction was chosen as the quantitative indicator of the outer membrane permeabilization.

To test cytoplasmic membrane permeability, 0.7 g L<sup>-1</sup> ONPG was added to each sample solution. The cytoplasmic membrane permeabilization was revealed by ONPG hydrolysis due to the cytoplasmic  $\beta$ -galactosidase. The hydrolysis product of ONPG (ONP) was detected by absorbance measurement at 420 nm (Multiscan Go, Thermo Fisher Scientific, Illkirch, France) at 37°C under stirring. The maximal velocity of the enzymatic reaction was chosen as the quantitative indicator of the cytoplasmic membrane permeabilization.

These membrane permeabilization tests were performed in triplicate.

## 2.10 | Detection of $\beta$ -lactamase and $\beta$ -galactosidase leakage out of bacteria cells

The method for the detection of  $\beta$ -lactamase and  $\beta$ -galactosidase leakage was based on a method proposed by Derde et al. allowing the detection of pore formation in the outer and cytoplasmic membranes, respectively.<sup>[4]</sup> Briefly, the *E. coli* ML-35p culture was grown overnight (18 h) in TSB containing 50  $\mu$ g mL<sup>-1</sup> ampicillin at 37°C under stirring (130 rpm). After twice-washed in 50 mM Tris-HCl buffer pH 7.0, the bacterial culture was diluted to obtain about 10<sup>7</sup> CFU mL<sup>-1</sup> bacteria suspensions in which lysozyme was added (3.7 g L<sup>-1</sup> DH-L, 0.19 g L<sup>-1</sup> ISO-L, 1.9 g L<sup>-1</sup> NL-L or 1.7 g L<sup>-1</sup> SUC-L) before incubation for 5 h at 37°C under stirring, and then centrifugation at 5000g for 10 min.  $\beta$ -lactamase and  $\beta$ -galactosidase activities were then tested in the supernatants by adding 0.05 g L<sup>-1</sup> nitrocefin and 1 g L<sup>-1</sup> ONPG, respectively. The initial reaction rates of both enzymatic reactions ( $v_0 = \Delta AU/\text{min}$ ) were determined at 25°C from absorbance curves (Multiscan Go, Thermo Fisher Scientific, Illkirch, France) at 486 and 420 nm, respectively. The results were based on three replicates.

## 2.11 | Measurement of the bacterial membrane potential dissipation

The dissipation of the bacterial membrane potential was measured according to the method proposed by Wu et al.<sup>[20]</sup> The *E. coli* K12 culture was grown for 3.5 h in TSB at 37°C under stirring (130 rpm) in order to reach a mid-log phase. After twice-washed with 5 mM HEPES-buffer at pH 7.2 and containing 5 mM glucose (5000g, 10 min), the bacteria suspension was diluted to reach an absorbance around 0.06 at 620 nm, and 1  $\mu$ M DiSC<sub>3</sub> and 100 mM KCl were added before incubation for 1 h at 30°C in the dark. Then, lysozyme (3.7 g L<sup>-1</sup> DH-L, 0.19 g L<sup>-1</sup> ISO-L fraction, 1.9 g L<sup>-1</sup> NL-L fraction or 1.7 g L<sup>-1</sup> SUC-L fraction) was added to the bacteria suspension before incubation for 30 min at 30°C in the dark. Fluorescence was then measured at 670 nm with a fluorimeter Perkin Elmer LS55 (Perkin Elmer, Courtaubeuf, France), after excitation at 622 nm; slit width was 2.5/2.5 and

integration time was 6.2 s. The results were based on six replicates (two biological replicates, each with three technical replicates).

## 2.12 | Lipid monolayers and surface pressure measurements

The experiments were performed in a homemade 8 mL Teflon trough previously and thoroughly cleaned with successively warm tap water, ethanol, demineralized water and then boiled for 15 min. To prepare lipid monolayers, the trough was filled with 8 mL HEPES-buffer, on which LPS or CMEC were spread with a high precision Hamilton micro-syringe until to obtain an initial surface pressure around 20 mN m<sup>-1</sup>. After 1 h or 15 min of solvent evaporation for LPS or CMEC, respectively, 50  $\mu$ L of DH-L, ISO-L, NL-L, or SUC-L solutions were injected in the subphase with a Hamilton syringe until a final protein concentration of 1.4 mg L<sup>-1</sup> was reached. This concentration has been chosen in the linear zone of  $\Delta\pi$  versus protein concentration plot observed for LPS/lysozyme and CMEC/lysozyme interactions (data not shown), in order to avoid protein aggregation in the bulk solution, while enabling the evaluation of lipid-protein interactions. Thus, the proportional concentrations of the isoforms as they are naturally present in the DH-L mixture cannot be tested, because of the previously explained technical limits; DH-L and lysozyme isoforms were all tested at 1.4 mg L<sup>-1</sup>.

The surface pressure was measured following a Wilhelmy method using a 10 mm  $\times$  22 mm filter paper as plate (Whatman, Velizy-Villacoublay, France) connected to a microelectronic feedback system (Nima PS4, Manchester, England). The surface pressure ( $\pi$ ) was recorded every 4 s until equilibrium was reached; the precision was  $\pm 0.2$  mN m<sup>-1</sup>. The results were based on three replicates.

## 2.13 | Statistical data analysis

Statistical analysis was performed with R 3.0.3. Data from the normal distribution and with equal variances were treated with parametric tests. The ANOVA Tukey multiple comparisons were then used for the comparison of means. Data from other distributions or with unequal variances were treated with non-parametric tests. The Wilcoxon rank sum test was then used for the comparison of means. Differences described in this manuscript were significant with  $P < 0.05$ .

# 3 | RESULTS

## 3.1 | Preparation and characterization of the enriched fractions of lysozyme isoforms

The limits determined to discriminate between the different lysozyme isoforms when dry-heated lysozyme (DH-L) is analyzed by cation exchange high pressure liquid chromatography (CE-HPLC) have been determined according to Desfougères et al.<sup>[14]</sup> Thus, DH-L consists of a mixture of 7% isoaspartyl lysozyme, 49% native-like lysozyme, and 44% succinimide lysozyme (Figure 1). Three lysozyme fractions enriched respectively in isoaspartyl isoform (ISO-L fraction), native-like isoform (NL-L fraction), and succinimide isoform (SUC-L fraction) have been purified from DH-L by cation exchange chromatography on a



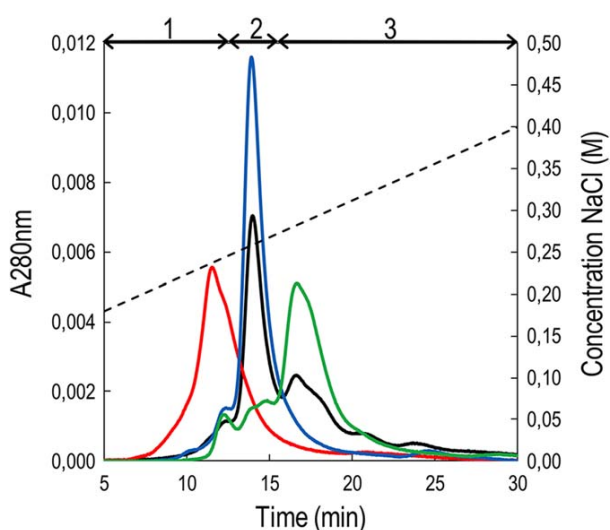


**FIGURE 1** Cation exchange HPLC on S-HYPER D10 in 20 mM acetate buffer pH 5.0 of 1 mg mL<sup>-1</sup> DH-L (black line), ISO-L (red line), NL-L (blue line) and SUC-L (green line) fractions. ISO-L, NL-L and SUC-L fractions were collected as indicated with 1, 2, and 3, respectively

pilot scale, and using the latter limits. Cation exchange chromatography was selected since it is a poorly denaturing method, relevant for preparative scale purification, and knowing that the apparent net charge is the most significant difference between the isoforms. The analysis by CE-HPLC of the collected fractions enabled to estimate their composition as follows: ISO-L fraction consists of 100% isoaspartyl lysozyme, NL-L fraction consists of 9% isoaspartyl lysozyme and 91% native-like lysozyme, and SUC-L fraction consists of 7% isoaspartyl lysozyme, 14% native-like lysozyme and 78% succinimide lysozyme (Figure 1). Thus, despite a purity lower than 100%, these both latter fractions are strongly enriched with native-like and succinimide isoforms, respectively, compared to the initial DH-L mixture.

Structure analysis of these different fractions has been performed combining different methods. Circular dichroism (CD) analysis in the near UV shows no significant conformational change between the fractions (Figure 2E). However, intrinsic fluorescence analysis of tryptophyl residues (4 Trp residues located in disordered regions and 1 in a  $\alpha$ -helix) indicates a slight increase of the maximal emission wavelength (2 nm red shift) for SUC-L and ISO-L fractions as compared to NL-L fraction (Figure 2A). Thus, Trp residues would be more solvent-exposed in SUC-L and ISO-L fractions, suggesting a slight modification of their tertiary structure compared to NL-L fraction. This is consistent with the ANS fluorescence, which shows a decrease of the maximal emission wavelength (5 nm blue shift) for SUC-L and ISO-L fractions compared to NL-L fraction (Figure 2B). This suggests a higher surface hydrophobicity for the chemically modified isoforms of lysozyme, compared to the native-like isoform. The increased solvent-accessibility of the protein structure in SUC-L and ISO-L fractions could favor the binding of ANS to hydrophobic patches. Finally, regarding the secondary structures, the CD spectra in the far UV shows two minima at 207

and 223 nm which are characteristic of polypeptides with high helical content, but no significant difference exists between NL-L, SUC-L, and ISO-L fractions (Figure 2D). This is consistent with the location of the amino acid residues which are modified by dry-heating, mainly in unstructured regions of lysozyme,<sup>[14]</sup> then, the lysozyme  $\alpha$ -helices and  $\beta$ -sheets should not be strongly affected. Similarly, no significant difference can be drawn from the infrared spectra for the amide I and amide II bands at 1650 and 1540 cm<sup>-1</sup>, respectively, indicative of  $\alpha$ -helix structures (Figure 2F). The only and main difference between the FTIR spectra concerns with the band at 1747 cm<sup>-1</sup> which can be attributed to keto-enol equilibrium and which appears more intense in ISO-L fraction compared to SUC-L and NL-L fractions (Figure 2F).

The molecular stability of the three enriched fractions has been investigated by differential scanning calorimetry. The transition temperature ( $T_m$ ) gives the temperature at which the number of folded and unfolded protein molecules is the same; it is thus representative of the protein stability. Data show that  $T_m$  is shifted to lower temperatures from NL-L fraction (76.3°C) to ISO-L fraction (75.1°C) and SUC-L fraction (73.9°C), while the enthalpy of the main transition ( $\Delta H$ ) does not significantly change (Table 1). These results indicate that SUC-L fraction is the least stable, and that ISO-L fraction is less stable than NL-L fraction. In addition, when fitted with a two-state scaled model, the transition peak appears symmetric and sharp for the NL-L isoform, showing the absence of unfolding intermediates. In contrast, the transition peaks are much broader for SUC-L and ISO-L fractions (Figure 2C), consistently with the heterogeneity of these fractions which are mixtures of different levels of chemical modifications (from 1 up to 5 modified amino acid residues per lysozyme molecule). For these chemically modified isoforms, the transition peaks are well fitted using two independent two-state models, suggesting two successive unfolding events (Table 1). The higher  $T_m$  ( $T_{m1}$ ) is close to the one observed for native lysozyme whereas the lower  $T_m$  ( $T_{m2}$ ) could be the consequence of the destabilization induced by the chemical modifications. SUC-L fraction is the most affected with the lowest temperature event contributing to almost 50% of the protein unfolding. Altogether, the global impact of the chemical modifications on lysozyme stability could appear rather weak, with <3°C difference between the most and the least stable isoforms. Actually, this impact is very high with respect to the few number of chemical modifications (from 1 up to 5) compared to the total number of amino acid residues of lysozyme (129).

Otherwise, protein adsorption at the air/liquid interface was measured in order to estimate the amphiphilicity of each lysozyme fraction. Surface pressure increase is indicative of the protein ability to expose hydrophobic patches at the interface. While SUC-L fraction results in a surface pressure increase of  $12.9 \pm 0.4$  mN m<sup>-1</sup>, ISO-L and NL-L fractions lead to a lower increase of  $3.0 \pm 0.6$  mN m<sup>-1</sup> (Table 2).

### 3.2 | Growth of *E. coli* K12 in the presence of DH-L and fractions

To estimate the antimicrobial activity of DH-L and its fractions, *E. coli* K12 growth assays were performed in the presence of the different lysozyme fractions. Native lysozyme (N-L) and DH-L were tested at

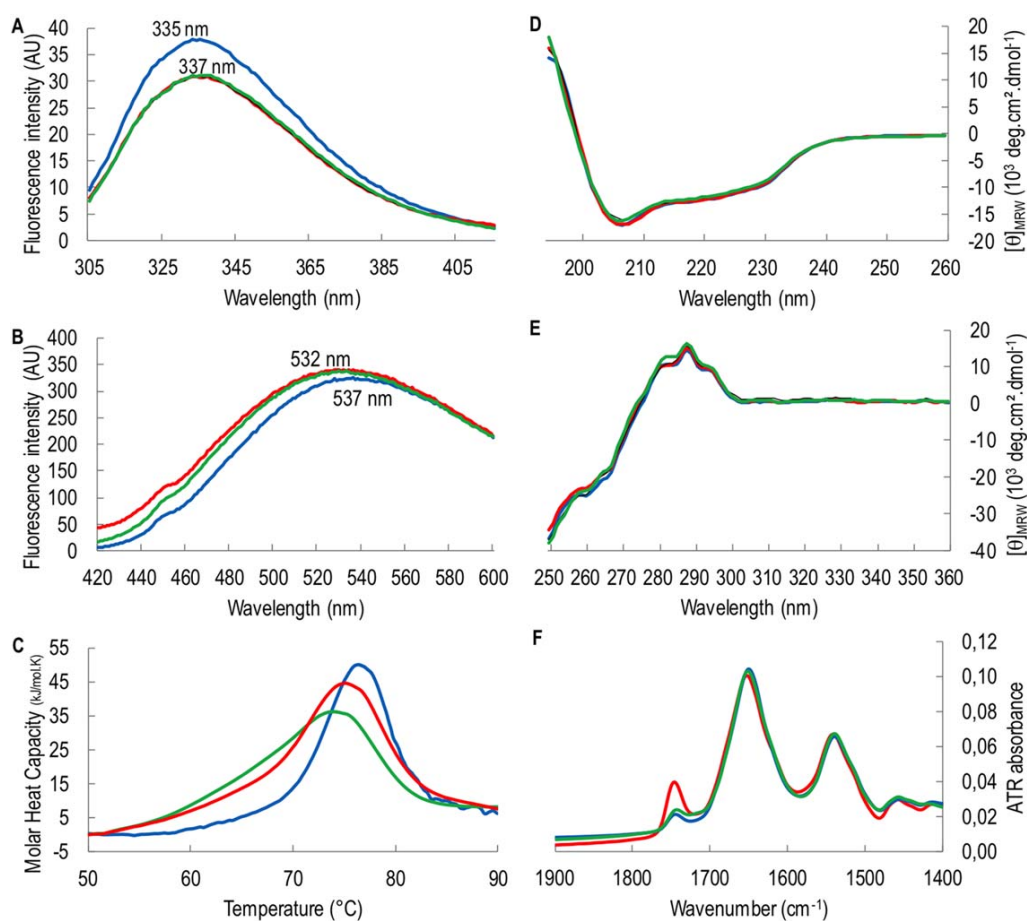


**FIGURE 2** Optical spectroscopy analysis of secondary and tertiary structures, infrared spectroscopy analysis, and differential scanning calorimetry analysis of ISO-L (red line), NL-L (blue line) and SUC-L (green line) fractions. (A) Intrinsic fluorescence after excitation at 295 nm; (B) surface hydrophobicity assessed by ANS fluorescence after excitation at 390 nm; (C) nano-differential scanning calorimetry in the 50–90°C range; circular dichroism analysis in the far (D) and near UV (E); (F) infrared spectroscopy analysis in the 1400–1900  $\text{cm}^{-1}$  range

$3.7 \text{ g L}^{-1}$ , the natural concentration of lysozyme in hen egg white. To mimic the relative proportions of isoforms originally determined in DH-L, the fractions were tested at  $0.19$ ,  $1.9$ , and  $1.7 \text{ g L}^{-1}$  for ISO-L, NL-L and SUC-L, respectively, that is, 5, 50, and 45% of  $3.7 \text{ g L}^{-1}$ .

The control sample, without addition of lysozyme, and ISO-L fraction enable *E. coli* growth resulting in respectively  $+1.3 \text{ logCFU mL}^{-1}$  and  $+0.5 \text{ logCFU mL}^{-1}$  after 2-h incubation (Figure 3). In contrast, DH-L and SUC-L fraction induce a population decrease after 2-h incubation, resulting in  $-1.0 \text{ logCFU mL}^{-1}$  and  $-0.6 \text{ logCFU mL}^{-1}$ ,

**TABLE 1** Thermodynamic parameters obtained for NL-L, ISO-L, and SUC-L fraction unfolding measured by NanoDSC, and fitted with a two-state scaled model

|       | Measured   |                                     | Model         |                                       |               |                                       |
|-------|------------|-------------------------------------|---------------|---------------------------------------|---------------|---------------------------------------|
|       | $T_m$ (°C) | $\Delta H$ ( $\text{kJ mol}^{-1}$ ) | $T_{m1}$ (°C) | $\Delta H_1$ ( $\text{kJ mol}^{-1}$ ) | $T_{m2}$ (°C) | $\Delta H_2$ ( $\text{kJ mol}^{-1}$ ) |
| NL-L  | 76.33      | 366                                 | 76.30         | 365                                   | -             | -                                     |
| ISO-L | 75.08      | 366                                 | 75.46         | 278                                   | 69.17         | 94                                    |
| SUC-L | 73.94      | 372                                 | 74.63         | 203                                   | 67.58         | 191                                   |

respectively (Figure 3). DH-L is thus the most efficient lysozyme sample for *E. coli* destruction. The slight population decrease observed with NL-L fraction ( $-0.3 \text{ logCFU mL}^{-1}$ ) does not significantly differ from that observed with N-L ( $-0.2 \text{ logCFU mL}^{-1}$ ) after 2-h incubation (Figure 3).

**TABLE 2** Surface pressure increase ( $\Delta\pi$ ) at the air interface and rate constant of adsorption ( $k_{\text{ads}}$ ) at the air, LPS monolayer, and CMEC monolayer interfaces after injection in the subphase of  $1.4 \text{ mg L}^{-1}$  DH-L, ISO-L, NL-L, and SUC-L fractions

|   | DH-L          | ISO-L          | NL-L          | SUC-L          |
|---|---------------|----------------|---------------|----------------|
| $\Delta\pi$ ( $\text{mN m}^{-1}$ )                        |               |                |               |                |
| Air/liquid  | $11 \pm 1$    | $3 \pm 0.3$    | $3.2 \pm 0.6$ | $12.9 \pm 0.4$ |
| $k_{\text{ads}}$ ( $10^3 \text{ M}^{-1} \text{ s}^{-1}$ ) |               |                |               |                |
| Air/liquid  | $0.8 \pm 0.2$ | $0.9 \pm 0.1$  | $0.5 \pm 0.1$ | $1.3 \pm 0.3$  |
| LPS/liquid  | $1.3 \pm 0.1$ | $1.5 \pm 0.0$  | $2.3 \pm 0.4$ | $1.4 \pm 0.4$  |
| CMEC/liquid   | $5.5 \pm 0.3$ | $30.0 \pm 0.3$ | $5.0 \pm 0.4$ | $11.6 \pm 0.4$ |

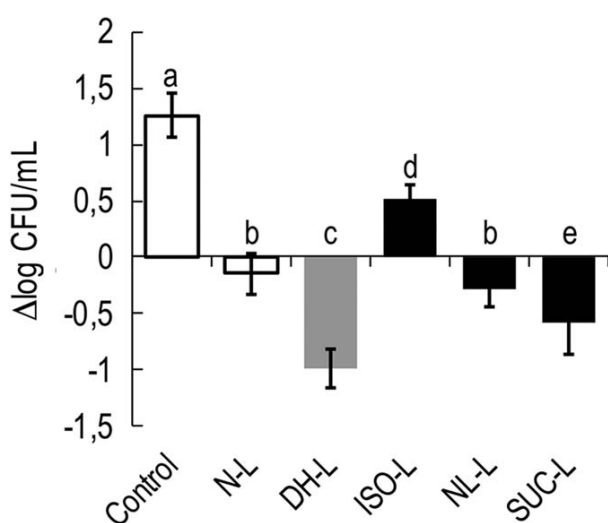


**FIGURE 3** *E. coli* K12 growth or destruction after 2-h incubation at 37°C in the absence (control sample) and the presence of 3.7 g L<sup>-1</sup> N-L, 3.7 g L<sup>-1</sup> DH-L, 0.19 g L<sup>-1</sup> ISO-L, 1.9 g L<sup>-1</sup> NL-L and 1.7 g L<sup>-1</sup> SUC-L. Different letters indicate significant difference obtained from the ANOVA analysis combined with Tukey multiple comparisons ( $n = 9$ ,  $P < 0.05$ )

### 3.3 | Membrane state of *E. coli* ML-35p in the presence of DH-L and fractions

*E. coli* ML-35p is an *E. coli* mutant that allows the detection of the outer and cytoplasmic membrane permeabilization by enzymatic reactions of  $\beta$ -lactamase and  $\beta$ -galactosidase, respectively. The absorbance of the enzymatic reaction products is measured over time by spectrophotometry at 486 and 420 nm for the outer and cytoplasmic membrane permeabilization, respectively. The maximal slope of the absorbance versus time plot directly relates to the overall permeabilization of the bacterial cell membranes as described by Derde et al.<sup>[3]</sup> However, this enzymatic reaction can take place either only inside the cell by diffusion of the reactants from outside, or inside and outside the cell if the reactants and the enzymes diffuse through the cell membranes. To distinguish between these two possible situations, the amount of enzyme leakage has been evaluated as described by Derde et al.<sup>[3]</sup> The externalized enzyme activity is related to the amount and to the size of pores formed into the bacterial membrane.

DH-L and the ISO-L, NL-L, and SUC-L fractions induce an overall permeabilization of the outer membrane of *E. coli*, as evidenced by the overall  $\beta$ -lactamase activity (Figure 4A). It is noticeable that all the fractions permeabilize the outer membrane more severely than DH-L, and that SUC-L is the more efficient fraction (Figure 4A). Oppositely, the measurement of externalized  $\beta$ -lactamase activity highlights that DH-L is more efficient than each fraction separately to release the enzyme out of the bacteria cells (Figure 4B).

The overall permeabilization of the *E. coli* cytoplasmic membrane induced by DH-L is more severe than that induced by the fractions, as evidenced by  $\beta$ -galactosidase activity (Figure 5A). NL-L is proved to be

the less efficient fraction according to this criterion. It should be noticed that no externalized  $\beta$ -galactosidase activity could be detected for DH-L or its fractions (data not shown). The cytoplasmic membrane state was also investigated by the measurement of membrane potential dissipation. It shows that DH-L disturbs the membrane potential more strongly than each fraction, and that ISO-L induces the lowest disturbance compared to the other fractions (Figure 5B).

### 3.4 | Interaction of DH-L and fractions with outer and cytoplasmic membrane models

To investigate the molecular interactions of DH-L and each fraction with the *E. coli* membrane lipids, monolayer models were used. To mimic the *E. coli* outer membrane, the lipid monolayer consisted of lipopolysaccharides (LPS) extracted from *E. coli* K12. To mimic the *E. coli* cytoplasmic membrane, the lipid monolayer consisted of a phospholipid mixture with a lipid composition based on the analysis of *E. coli* cytoplasmic membrane (CMEC) performed by Lugtenberg and Peters.<sup>[16]</sup> The lipids were spread at the buffer surface until 20 mN m<sup>-1</sup> lateral surface pressure was reached. This initial surface pressure was chosen based on similar experiments performed by Zhang et al.,<sup>[21]</sup> Gidalevitz et al.,<sup>[22]</sup> and Coccia et al.<sup>[23]</sup>

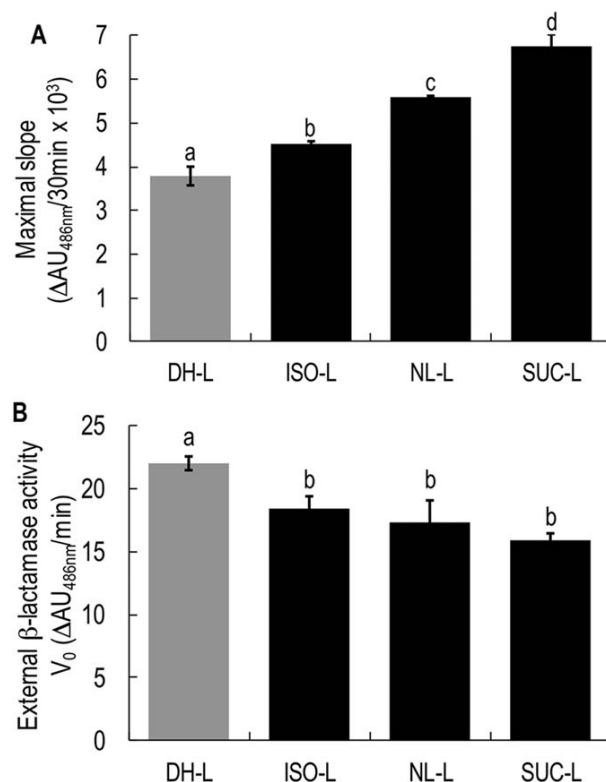


**FIGURE 4** Permeabilization of the *E. coli* ML-35p outer membrane by 3.7 g L<sup>-1</sup> DH-L, 0.19 g L<sup>-1</sup> ISO-L, 1.9 g L<sup>-1</sup> NL-L or 1.7 g L<sup>-1</sup> SUC-L as evidenced by the overall (A) and externalized (B)  $\beta$ -lactamase activity. Different letters indicate significant difference obtained from the ANOVA analysis combined with Tukey multiple comparisons ( $n = 3$ ,  $P < 0.05$ )



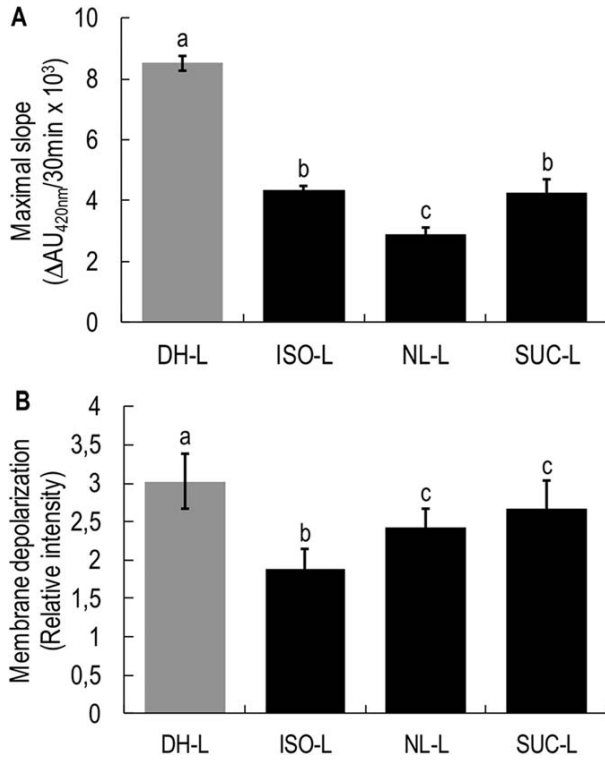


**FIGURE 5** Permeabilization of the *E. coli* ML-35p cytoplasmic membrane as evidenced by the  $\beta$ -galactosidase activity (A) and dissipation of the membrane potential of *E. coli* K12 (B) induced by  $3.7 \text{ g L}^{-1}$  DH-L,  $0.19 \text{ g L}^{-1}$  ISO-L,  $1.9 \text{ g L}^{-1}$  NL-L, or  $1.7 \text{ g L}^{-1}$  SUC-L. Different letters indicate significant difference obtained from the ANOVA analysis combined with Tukey multiple comparisons ( $n = 3$ ,  $P < 0.05$ )

A surface pressure increase ( $\Delta\pi$ ) after lysozyme injection into the subphase indicates that lysozyme inserts into the lipid monolayer. The lysozyme concentration used for these experiments was  $1.4 \text{ mg L}^{-1}$  regardless the sample, for technical reasons explained in the experimental procedures section.

The surface pressure increase after DH-L injection indicates that DH-L inserts into the LPS monolayer and into the CMEC monolayer. Moreover DH-L inserts more efficiently into both LPS (Figure 6A) and CMEC (Figure 6B) monolayers compared to all the fractions, except SUC-L fraction that is as efficient as DH-L regarding LPS monolayer. Among the fractions, SUC-L induces higher  $\Delta\pi$  values than NL-L and ISO-L fractions in LPS monolayer (Figure 6A), whereas NL-L and SUC-L fractions are equivalent in CMEC monolayer (Figure 6B).

The rate constants of adsorption ( $k_{\text{ads}}$ ) of DH-L and lysozyme isoforms solutions with a concentration ( $c$ ) of  $1.4 \text{ mg L}^{-1}$  at the air/liquid interface, at the LPS/liquid interface, and at the CMEC/liquid interface have been evaluated by fitting experimental adsorption data to the Langmuir equations (Equations 2 and 3). The rate constants of desorption  $k_{\text{des}}$  can be considered negligible for the fractions when estimating that their interfacial behavior is comparable to DH-L for which desorption is negligible (data not shown).

$$\pi(t) = \pi_{\text{final}}(1 - e^{-\sigma t}) \quad (2)$$

$$\sigma = k_{\text{ads}}c + k_{\text{des}} \quad (3)$$

The  $k_{\text{ads}}$  values are systematically lower (or equivalent) at the air/liquid interface as compared to LPS/liquid and CMEC/liquid interfaces (Table 2). Thus, regardless the sample, lysozyme adsorption is slower at the air/liquid interface; suggesting lysozyme has higher affinities for the LPS and CMEC monolayers. Moreover, it is noticeable that significantly higher values of  $k_{\text{ads}}$  are measured at the CMEC/liquid interface, as compared to the LPS/liquid interface. At last, significantly different adsorption rates at the CMEC monolayer are observed between the fractions: ISO-L fraction adsorbs much more quickly than SUC-L fraction, whereas DH-L and NL-L fraction are the slowest for adsorption at the CMEC monolayer (Table 2). In contrast, the adsorption rates at the LPS monolayer were not significantly different for DH-L, ISO-L and SUC-L fractions, whereas a slightly higher value is obtained for NL-L fraction.

## 4 | DISCUSSION

The enhanced effect of DH-L compared to N-L on the *E. coli* outer and cytoplasmic membranes was previously established by Derde et al.<sup>[4]</sup>

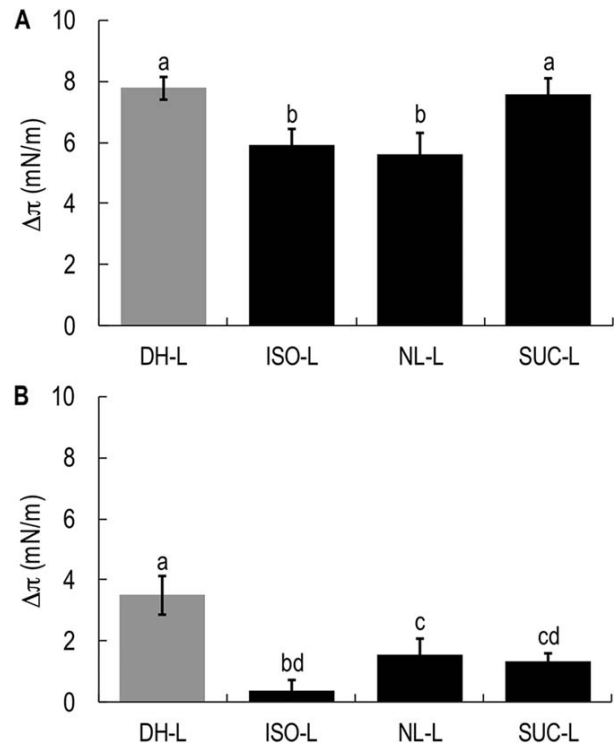


**FIGURE 6** Overpressure ( $\Delta\pi$ ) induced by insertion of DH-L or its fractions into a LPS monolayer (A) and into a CMEC monolayer (B) after a subphase injection of  $1.4 \text{ mg L}^{-1}$  lysozyme. The initial surface pressure ( $\pi_{\text{initial}}$ ) was  $20 \text{ mN m}^{-1}$  for both monolayers. Different letters indicate significant difference obtained from the ANOVA analysis combined with Tukey multiple comparisons ( $n = 3$ ,  $P < 0.05$ )

DH-L creates pores in the outer membrane, and strongly affects the cytoplasmic membrane as evidenced by an increased permeability and membrane potential dissipation. It can be assumed that it results from the modified physicochemical properties of DH-L compared to native lysozyme. However, DH-L is actually a mixture of different isoforms: isoaspartyl lysozyme, native-like lysozyme, and succinimide lysozyme, each exhibiting specific physicochemical properties.<sup>[15]</sup> Thus, the question arises of the relative involvement of each isoform in the increased antibacterial activity of DH-L, and of the decisive features which make some isoforms more efficient than others. To answer these questions, the present study aimed to evaluate the antimicrobial and membrane activity of each lysozyme isoform induced by dry-heating, and to relate such activities and molecular properties. Further, these isoforms were also compared to DH-L regarding antimicrobial and membrane activities.

#### 4.1 | Flexibility, as well as the positive net charge and hydrophobicity, is a key parameter for the membrane activity of the lysozyme isoforms

At a physiological pH, the three lysozyme isoforms are positively charged. Then, positive charge of proteins and peptides is reported as an important prerequisite for interaction with bacterial membranes, and eventually for antimicrobial activity.<sup>[2,24]</sup> But ISO-L, NL-L, and SUC-L isoforms differ in apparent net charge as shown by cation exchange chromatography (Figure 1). And it is noticeable that SUC-L fraction, which contains the isoform with the highest positive charge at neutral pH, exhibits the highest outer membrane activity *in vivo* (Figure 4A) and *in vitro* (Figure 6A). SUC-L fraction also permeabilizes more efficiently the cytoplasmic membrane compared to the NL-L fraction (Figure 5A), and SUC-L fraction adsorbs more rapidly at the CMEC monolayer than the NL-L fraction (Table 2), even though insertion into the CMEC monolayer is similar for both fractions (Figure 6B). The attraction of the highly positively charged SUC-L isoform for the negatively charged cytoplasmic membrane could be responsible for the more rapid adsorption to the membrane surface and the higher permeabilization. Thus, the positive charge of SUC-L isoform could be related to the higher efficiency of the SUC-L fraction for membrane disruption, and then for bacteria destruction since severe membrane disruption can lead to bacteria cell death.<sup>[20,25]</sup> The antimicrobial activity of the lysozyme fractions appears thus correlated with the charge of the isoforms. When SUC-L, NL-L, and ISO-L fractions are compared, the higher the positive charge, the higher the antimicrobial activity. Moreover, NL-L fraction and native lysozyme, equally charged as evidenced by their simultaneous elution in cation exchange chromatography (data not shown),<sup>[14]</sup> exhibit equivalent antimicrobial activity (Figure 3).

Additionally, the lysozyme isoforms not only differ in positive charge, but also in hydrophobicity. Especially, SUC-L fraction is more hydrophobic than NL-L fraction (Figure 2B), which is consistent with the higher antimicrobial activity of SUC-L fraction (Figure 3). It should be noticed that the blue shift observed for SUC-L and ISO-L fractions compared to NL-L fraction when ANS fluorescence is measured (Figure 2B), suggests a still higher blue shift for the SUC-L isoform,

since SUC-L fraction contains 7% ISO-L and 14% NL-L isoforms. In other words, SUC-L isoform is not only more hydrophobic than NL-L isoform, but probably also more hydrophobic than ISO-L isoform. Anyway, while the ANS study indicates an equivalent hydrophobicity for SUC-L and ISO-L fractions (Figure 2B), the ability to expose hydrophobic patches is higher for SUC-L fraction than for ISO-L fraction, as indicated by the higher surface pressure increase when SUC-L fraction adsorbs at air-water interface. This could explain that ISO-L fraction does not exhibit any bactericidal activity, unlike SUC-L fraction (Figure 3).

The molecular flexibility would be another key parameter that distinguishes between the fractions, SUC-L fraction being the most flexible one (Figure 2C, Table 1). It is noticeable that, despite the presence of 7% ISO-L and 14% NL-L isoforms in SUC-L fraction, this latter appears significantly more flexible than ISO-L and NL-L fractions. This suggests that SUC-L isoform is much more flexible than NL-L and even than ISO-L isoforms. Then, flexible protein would be more prone to the conformational changes necessary for membrane/protein interactions,<sup>[26]</sup> especially by displaying hydrophobic patches.

Then, SUC-L isoform is not only the most positively charged, but would be also the most hydrophobic and the most flexible isoform. Moreover, when compared at the same concentration, SUC-L fraction results in a surface pressure increase at the air-water interface fourfold higher than that resulting from ISO-L and NL-L fractions (Table 2), and significantly higher at the LPS-water interface (Figure 6A). In the same way, when the fractions are compared at different concentrations, representative of the concentrations naturally observed in DH-L mixture, SUC-L fraction proved to be the most efficient for the permeabilization of the *E. coli* outer membrane (Figure 4A). Because SUC-L fraction is more surface active than NL-L and ISO-L fractions, and knowing that neither NL-L nor ISO-L fractions contain SUC-L isoform, while SUC-L fraction contains small percentages of NL-L and ISO-L isoforms, it can then be assumed that the highest efficiency of SUC-L fraction can be ascribed to SUC-L isoform.

However, and despite a lower positive charge and at much lower concentration, ISO-L fraction is as efficient as SUC-L fraction regarding cytoplasmic membrane permeabilization, and more efficient than NL-L fraction (Figure 5A). Moreover, ISO-L fraction has the highest adsorption rate onto the negative CMEC monolayer (Table 2), whereas it is the less basic isoform. It could be assumed that besides electrostatic attraction, diffusion kinetics can play a role. Then, protein diffusion depends on the friction coefficient determined by the protein size and shape.<sup>[27]</sup> Because ISO-L fraction is more stable than SUC-L fraction as indicated by  $T_m$  values (Table 1), it is thus imaginable that isoaspartyl lysozyme is a more compact protein than succinimide lysozyme. Then, ISO-L would diffuse more quickly to the cytoplasmic membrane despite slightly lower electrostatic attractions.

Strikingly, it should be noticed that despite the high rate of adsorption of ISO-L fraction onto CMEC monolayer (Table 2), this fraction poorly inserts between the CMEC lipids (Figure 6B). ISO-L fraction is thus adsorbing onto the lipid monolayer, but remains beneath the latter. It can be assumed that the structure stability of ISO-L isoform

does not allow the needed structural changes for insertion between the phospholipids, unlike the highly flexible SUC-L isoform. However, ISO-L fraction is able to permeabilize the cytoplasmic membrane, even at low concentration (Figure 5A). Protein insertion is thus not a prerequisite for membrane permeabilization. An assumption could be that ISO-L adsorption onto the cytoplasmic membrane induce lipid clustering leading to membrane permeabilization, similarly to what has been already described for magainin analogs and arginine-rich peptides.<sup>[28]</sup>

These results emphasize the complexity of the phenomena leading to the interaction between lysozyme and bacterial membranes. But clearly, slight physicochemical differences such as those discriminating isoaspartyl, native-like and succinimide lysozymes suffice to induce different interactions with bacterial membranes. And protein flexibility seems to play a key role in these phenomena, when the protein presents also a positive net charge and high hydrophobicity.

## 4.2 | Antimicrobial activity of DH-L results from the complementarity between the lysozyme isoforms

Bacteria counts after 2-h incubation in the presence of lysozyme show that DH-L has a higher antimicrobial effect on *E. coli* than each fraction (Figure 3). This result demonstrates that the DH-L effect on *E. coli* cells is not due to one single isoform. Actually, DH-L is an efficient mixture of complementary isoforms.

The cooperation of the DH-L isoforms is also observed when evaluating the DH-L effect on the *E. coli* membranes. Both DH-L and its fractions disrupt the outer and cytoplasmic membranes of *E. coli* (Figures 4 and 5), with and without pore formation, respectively. When comparing the effect of DH-L and its fractions on the outer membrane, it can be noticed that DH-L causes a higher externalization of  $\beta$ -lactamase than its fractions (Figure 4B). This result proves that DH-L disrupts the outer membrane in such a way that  $\beta$ -lactamase, an enzyme of 28.9 kDa, can leak out of the periplasm in a larger extent than that induced by each fraction. In contrast, the three fractions cause a higher overall permeabilization of the outer membrane (Figure 4A). In other words, the three fractions induce a higher porosity than DH-L, but the created pores would be smaller resulting in limited enzyme diffusion. Hence, the results suggest that the three fractions would form a high number of small pores compared to DH-L that would form a small number of large pores. Despite a lower overall permeabilization due to DH-L compared to its fractions, the bacterial population decrease (Figure 3) is more severe with DH-L, suggesting that damages caused by few large pores are more deleterious for the bacteria cells than multiple small pores.

Similarly, the cytoplasmic membrane is more severely disrupted by DH-L compared to its fractions as shown by  $\beta$ -galactosidase activity and membrane potential measurements (Figure 5). It is noticeable that, opposite to outer membrane perforation, no pore formation into the cytoplasmic membrane by DH-L or its fractions has been detected.

Thus, the in vivo experiments suggest that the combination of lysozyme isoforms is needed to obtain an efficient outer and cytoplasmic membrane disruption. To confirm this hypothesis of cooperation between the different lysozyme isoforms, the LPS and

CMEC monolayer models have been used. These membrane models give us a higher understanding of the molecular interaction mechanisms between the antimicrobial protein and bacterial membranes.

DH-L and each fraction insert into both monolayers, and at equal concentration ( $1.4 \text{ mg L}^{-1}$ ), DH-L inserts more or equally than each fraction, regardless the monolayer nature (Figure 6). It should be noticed that each isoform consists only of 5–50% of the DH-L mixture. The  $\Delta\pi$ -values corresponding to each fraction would thus be lower than those here measured if tested at the concentrations representative of those originally found in DH-L. In other words, the  $\Delta\pi$ -values measured for ISO-L, NL-L, and SUC-L fractions (Figure 6) are overestimated as compared to the  $\Delta\pi$ -value induced by DH-L mixture. Thus, DH-L insertion into LPS and CMEC monolayers clearly results from cooperation between the different lysozyme isoforms. Because of the complexity of the phenomena here investigated, no direct measurement or observation could be done. But assumptions can be proposed to explain the higher efficiency of the DH-L mixture. Especially, the cooperative effect, which is the most pronounced for the CMEC monolayer, could be due to the differences in  $k_{\text{ads}}$  measured for each fraction (Table 2). ISO-L fraction, with the highest  $k_{\text{ads}}$ , would adsorb first onto the CMEC monolayer. This adsorption of isoaspartyl lysozyme onto the CMEC monolayer could then modulate the membrane in such a way that the adsorption and insertion of native-like and succinimide lysozymes are facilitated. This domino effect could then result in the cooperation highlighted in the DH-L mixture. Finally, both in vivo and in vitro experiments indicate a complementary effect between the lysozyme isoforms, which explains the higher efficiency of DH-L on *E. coli* cells.

## 5 | CONCLUSIONS

This study suggests that the positive net charge is one of the key parameters in the interaction between the isoforms of dry-heated lysozyme and bacterial membranes, in vivo and in vitro. Still, neither hydrophobicity nor molecular flexibility should be neglected. For example, succinimide lysozyme, the most positive, hydrophobic and flexible isoform, shows the highest antimicrobial activity against *Escherichia coli* and induces the strongest membrane disruption.

Another striking result is the complementary action of the isoforms present in DH-L, resulting in a higher antimicrobial activity of DH-L compared to individual fractions. Moreover, the bacterial membrane disruption caused by DH-L is generally more severe than that due to the fractions. A hypothesis is that the initial interaction of one of the isoforms with the bacterial membranes modifies the membrane characteristics in such a way to make insertion of the remaining isoforms easier, and thus increasing the impact on the membrane integrity. The damages caused by DH-L (isoform mixture) are then difficult to overcome by the bacteria and results in cell death.

Despite the advances made with this study for the understanding of the increased antibacterial activity of dry-heated lysozyme, many questions still arise. Especially, are conformational changes of the protein induced by its adsorption at lipid interface, and which changes?

Which part of the lysozyme molecule do insert into the lipid membranes? Methods such as PM-IRRAS could probably provide complementary data to answer these questions. Moreover, in order to get close to real biologic systems, native lysozyme and its derivative isoforms should be tested on membrane bilayers. And since the lipid composition of bacteria membranes strongly depends on bacteria species, this study encourages investigating the activity of DH-L and its isoforms on other Gram negative species. Depending on the results, some applications could be imagined, for food preservation or even medical uses. With this objective in mind, it could be also relevant looking for the optimal ratio of the three lysozyme isoforms, if this optimal ratio proves to be different from that naturally observed in DH-L mixture.

## ACKNOWLEDGMENTS

The authors thank "Conseil Régional de Bretagne" for the funding of this work, and thank Delphine Destoumieux-Garzon for kindly providing the *E. coli* ML-35p strain.

## AUTHOR CONTRIBUTIONS

M Derde conducted most of the experiments, analyzed the results, and wrote most of the article. MF Cochet contributed to the in vivo measurements of membrane permeability. G Paboeuf contributed to the in vitro measurements on lipid monolayers. M Pasco conducted spectroscopic and FTIR experiments under the supervision of S Pezennec who analyzed the results. S Sagan and A Walrant conducted the nano-DSC experiments and analyzed the results. V Lechevalier and C Guérin-Dubiard contributed to the scientific discussion and read over the article. F Baron, M Gautier and S Jan contributed to the experimental design and to the scientific discussion regarding the in vivo part. V Vié and F Nau conceived the idea for the project and wrote the article with M Derde.

## ORCID

Françoise Nau  <http://orcid.org/0000-0002-0167-8759>

## REFERENCES

- [1] World Health Organization, *Health Systems: improving performance*, 2000, XI–XVIII.
- [2] L. T. Nguyen, E. F. Haney, H. J. Vogel, *Trends Biotechnol.* **2011**, 29, 464.
- [3] M. Derde, V. Lechevalier, C. Guérin-Dubiard, M.-F. Cochet, S. Jan, F. Baron, M. Gautier, V. Vié, F. Nau, *J. Agric. Food Chem.* **2013**, 61, 9922.
- [4] M. Derde, C. Guérin-Dubiard, V. Lechevalier, M.-F. Cochet, S. Jan, F. Baron, M. Gautier, V. Vié, F. Nau, *J. Agric. Food Chem.* **2014**, 62, 1692.
- [5] A. Pellegrini, U. Thomas, R. von Fellenberg, P. Wild, *J. Appl. Bacteriol.* **1992**, 72, 180.
- [6] A. Pellegrini, U. Thomas, P. Wild, E. Schraner, R. Von Fellenberg, *Microbiol. Res.* **2000**, 155, 69.
- [7] Y. Mine, F. Ma, S. Lauriau, *J. Agric. Food Chem.* **2004**, 52, 1088.
- [8] H. Arima, H. R. Ibrahim, T. Kinoshita, A. Kato, *FEBS Lett.* **1997**, 415, 114.
- [9] H. R. Ibrahim, A. Kato, K. Kobayashi, *J. Agric. Food Chem.* **1991**, 39, 2077.
- [10] H. R. Ibrahim, M. Yamada, K. Matsushita, K. Kobayashi, A. Kato, *J. Biol. Chem.* **1994**, 269, 5059.
- [11] H. R. Ibrahim, S. Higashiguchi, L. R. Juneja, M. Kim, T. Yamamoto, *J. Agric. Food Chem.* **1996**, 44, 1416.
- [12] M. Derde, F. Nau, V. Lechevalier, C. Guérin-Dubiard, G. Paboeuf, S. Jan, F. Baron, M. Gautier, V. Vié, *Biochim. Biophys. Acta BBA Biomembr.* **2015**, 1848, 174.
- [13] M. Derde, F. Nau, C. Guérin-Dubiard, V. Lechevalier, G. Paboeuf, S. Jan, F. Baron, M. Gautier, V. Vié, *Biochim. Biophys. Acta BBA Biomembr.* **2015**, 1848, 1065.
- [14] Y. Desfougères, J. Jardin, V. Lechevalier, S. Pezennec, F. Nau, *Biomacromolecules* **2011**, 12, 156.
- [15] Y. Desfougères, A. Saint-Jalmes, A. Salonen, V. Vié, S. Beaufile, S. Pezennec, B. Desbat, V. Lechevalier, F. Nau, *Langmuir* **2011**, 27, 14947.
- [16] E. Lugtenberg, R. Peters, *Biochim. Biophys. Acta* **1976**, 441, 38.
- [17] H. Martens, J. P. Nielsen, S. B. Engelsen, *Anal. Chem.* **2003**, 75, 394.
- [18] F. Baron, M.-F. Cochet, W. Ablain, N. Grosset, M.-N. Madec, F. Gonnet, S. Jan, M. Gautier, *Le Lait* **2006**, 86, 251.
- [19] R. I. Lehrer, A. Barton, T. Ganz, *J. Immunol. Methods* **1988**, 108, 153.
- [20] M. Wu, E. Maier, R. Benz, R. E. W. Hancock, *Biochemistry (Mosc.)* **1999**, 38, 7235.
- [21] L. Zhang, A. Rozek, R. E. W. Hancock, *J. Biol. Chem.* **2001**, 276, 35714.
- [22] D. Gidalevitz, Y. Ishitsuka, A. S. Muresan, O. Kononov, A. J. Waring, R. I. Lehrer, K. Y. C. Lee, *Proc. Natl. Acad. Sci. USA* **2003**, 100, 6302.
- [23] C. Coccia, A. C. Rinaldi, V. Luca, D. Barra, A. Bozzi, A. Di Giulio, E. C. I. Veerman, M. L. Mangoni, *Eur. Biophys. J.* **2011**, 40, 577.
- [24] M. N. Melo, R. Ferre, M. A. Castanho, *Nat. Rev. Microbiol.* **2009**, 7, 245.
- [25] K. Matsuzaki, K. Sugishita, M. Harada, N. Fujii, K. Miyajima, *Biochim. Biophys. Acta BBA Biomembr.* **1997**, 1327, 119.
- [26] H. Jenssen, P. Hamill, R. E. W. Hancock, *Clin. Microbiol. Rev.* **2006**, 19, 491.
- [27] H. P. Erickson, *Biol. Proced. Online* **2009**, 11, 32.
- [28] R. M. Epand, R. F. Epand, *J. Pept. Sci.* **2011**, 17, 298.

**How to cite this article:** Derde M, Vié V, Walrant A, et al. Anti-microbial activity of lysozyme isoforms: Key molecular features. *Biopolymers*. 2017;e23040. <https://doi.org/10.1002/bip.23040>